

Mechanism of the Selective Catalytic Reduction of Nitric Oxide by Ammonia Elucidated by in Situ On-Line Fourier Transform Infrared Spectroscopy

Nan-Yu Topsøe

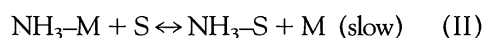
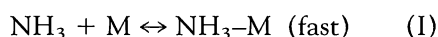
The selective catalytic reduction reaction of nitric oxide by ammonia over vanadia-titania catalysts is one of the methods of removing NO_x pollution. In the present study, it has been possible to identify the reaction mechanism and the nature of the active sites in these catalysts by combining transient or steady-state in situ (Fourier transform infrared spectroscopy) experiments directly with on-line activity studies. The results suggest a catalytic cycle that consists of both acid and redox reactions and involves both surface V–OH (Brønsted acid sites) and V=O species. A fundamental microkinetic model is proposed, which accounts for the observed industrial kinetics performance.

The emission of nitric oxide (NO) from power plants is a major environmental pollution issue. The most widely adopted method to combat this problem is the selective catalytic reduction (SCR) of NO by ammonia (NH₃) over vanadia-titania catalysts. However, despite extensive studies, the reaction mechanism and the nature of the active sites are still much debated (1–12).

In the SCR reaction, NO is converted to nitrogen according to the overall reaction



Recently Dumesic *et al.* (11) carried out a microkinetic analysis of the SCR reactions and found that the following type of semiempirical mechanism could model both the NO conversion and the important “NH₃ slip” (that is, the unreacted NH₃), which is a more sensitive measure of the activity than the conversion:



Briefly, this mechanism consists of a fast NH₃ adsorption step, a step involving activation of the adsorbed NH₃, followed by a reaction between the activated NH₃ and gaseous or weakly adsorbed NO to give the products. In this sequence of steps, M represents an NH₃ adsorption site and S is a reactive site involved in the activation of NH₃. The mechanism, although consistent with many observations (11), was still very speculative, and it was not possible to address the nature of the M and S sites or the nature of the reaction steps making up the complete catalytic cycle. In the present report, it will be shown that information about both the reaction steps and active surface

intermediates can be obtained by combining in situ Fourier transform infrared spectroscopy (FTIR) studies of the state of vanadia-titania catalysts with on-line mass spectrometric analysis of the reaction products.

The vanadia-titania catalysts were studied as self-supporting wafers of 100 mg in a quartz in situ infrared cell with CaF₂ windows (13). Gaseous bypass was minimized in this cell, and so the catalytic activities compared quite well with those obtained in separate plug-flow reactor studies. Before each temperature-programmed reaction experiment, the catalyst was oxidized in a mixture of 8% O₂ and 92% Ar at 400°C for 14 hours. The sample was then cooled to room temperature before switching from O₂ to flowing NH₃. Then NO or a mixture of NO and O₂ was subsequently passed over the NH₃-saturated catalyst surface while heating at a given temperature ramp (6°C per minute). For the SCR reaction studies, a gas mixture consisting of 500 ppm of NO, 500 ppm of NH₃, and 8% O₂ was passed over the oxidized catalyst at 250°C.

The first step that needs to be understood is the adsorption of NH₃. Earlier studies (1, 2, 9) have shown that both Brønsted acid sites (associated with V–OH surface groups) and Lewis acid sites are present in vanadia-titania catalysts. Although both types of sites are involved in NH₃ adsorption, it has not been established which type of sites is important in the catalytic reaction. This was addressed by use of the in situ on-line FTIR system where the changes in catalytic activity can be monitored simultaneously with the changes in the concentration of surface sites and adsorbed species. The results show a direct correlation between the concentration of the Brønsted acid sites (as indicated by the intensity of the NH₄⁺ band at 1430 cm⁻¹) and the NO_x conversion (Fig. 1). Clearly, no such correlation is seen for the Lewis acid

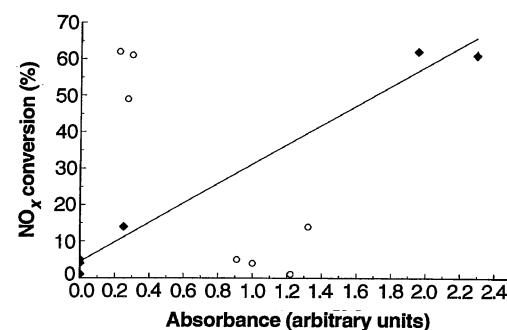


Fig. 1. Conversion of NO_x versus IR absorbance of NH₃ adsorbed on Brønsted (1430 cm⁻¹) (◆) and Lewis (1606 cm⁻¹) (○) acid sites on V₂O₅-TiO₂ catalysts with varying vanadia loadings.

sites. Thus, the Brønsted acid sites appear to be the catalytically important NH₃ adsorption sites.

Earlier studies (13) have shown that, of the reactants NH₃ and NO, only NH₃ is strongly adsorbed. Thus, one may obtain insight regarding the nature of the SCR reaction by exposing a catalyst with preadsorbed NH₃ to NO, or to a mixture of NO and O₂. It was found especially informative to carry out such experiments as temperature-programmed reaction studies. On exposure to either of these mixtures, NH₄⁺ species disappear from the surface with the simultaneous formation of N₂ and water in the gas phase. This result clearly indicates that the SCR reaction involves interaction of the preadsorbed NH₃ with NO.

The rate of disappearance of NH₄⁺ in flowing NO is slower than in NO + O₂, and this allows one to follow more conveniently the surface changes. During the temperature-programmed reaction studies, the in situ IR spectra (Fig. 2) show a progressive disappearance of the adsorbed NH₃ (bands at 3020, 2810, 1670, and 1430 cm⁻¹ are due to NH₄⁺ species, whereas bands at 3364, 3334, 3256, 3170, and 1602 cm⁻¹ are due to coordinated NH₃). The V–OH band

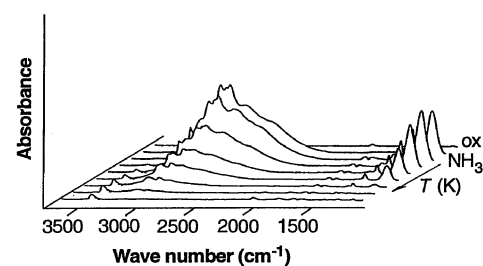


Fig. 2. In situ FTIR spectra of 6% V₂O₅-TiO₂ recorded during temperature-programmed reaction experiments in NO. The first and second spectra from the rear, respectively, were obtained at room temperature in a mixture of flowing O₂ and Ar before adsorption and in a mixture of flowing NH₃ and Ar. The subsequent spectra were obtained in flowing NO while heating from 100°C (with 50°C increments) to 350°C (front spectrum).

Haldor Topsøe Research Laboratories, DK-2800 Lyngby, Denmark.

(3640 cm^{-1}) gradually increases during this process. Some increase is not unexpected because the bands of these Brønsted acid sites were removed during the initial preadsorption of NH_3 . The expanded spectra in the OH region (Fig. 3A) also show that, above 200°C, the V–OH band at 3640 cm^{-1} becomes more intense than that seen on the sample before NH_3 adsorption. Furthermore, the position of the V–OH band shifts to higher wave numbers. These results indicate that the SCR reaction leads to the formation of new OH groups bonded to more reduced V centers. At higher temperatures (above 300°C), the intensity of this V–OH band decreases and the band returns to the position of the initially oxidized sample. These latter observations indicate that, after the initial reduction, reoxidation of the surface V species by NO has occurred at the elevated temperatures.

In addition to the V–OH surface sites, V=O groups also play an important role in the SCR reaction. Figure 3B shows that NH_3 adsorption leads to a downward frequency shift of the V=O band (2040 cm^{-1}) as reported in the literature (14, 15), reflecting a weakening of the V=O bond. This effect indicates that the V cations have undergone reduction, most probably by the transfer or partial transfer of H from the adsorbed NH_3 to the surface vanadyl groups to form an activated NH_3 species

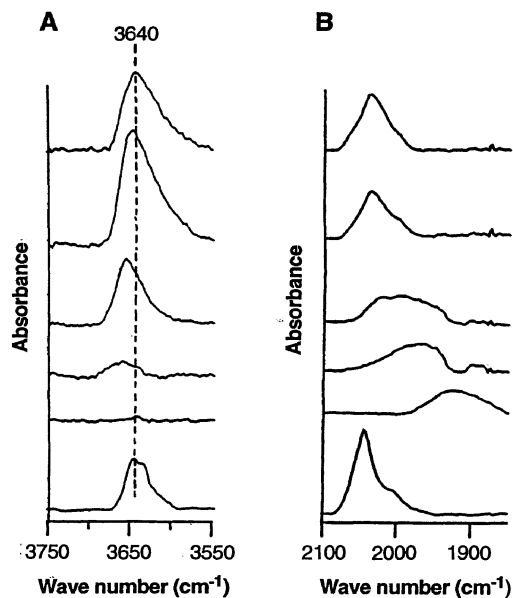
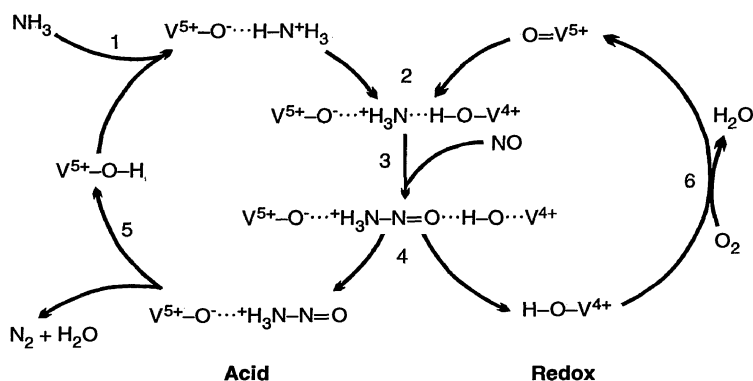


Fig. 3. FTIR spectra showing (A) the V–OH stretching band and (B) the V=O overtone band of 6% $\text{V}_2\text{O}_5\text{-TiO}_2$ during temperature-programmed reaction studies in NO (as in Fig. 2). The bottom spectra are spectra of the oxidized sample before NH_3 adsorption at room temperature. These are followed by the room temperature spectra in a mixture of flowing NH_3 and Ar and subsequently those in a mixture of NO and Ar at 100°, 200°, 300°, and 350°C. [The band due to NO gas has been subtracted from the spectra in (B).]



Scheme 1. Proposed scheme for the catalytic removal of environmental NO_x .

(that is, evidence for step II). The observed formation of new reduced V–OH species is consistent with this. These V=O groups could thus correspond to the S sites in the semiempirical model. Above 200°C, the original V=O groups reappear, which is also in line with the simultaneous changes seen in V–OH.

In summary, the above results indicate an initial reduction of $\text{V}^{5+}=\text{O}$ by interaction with the adsorbed NH_3 , which in turn becomes “activated” and more reactive toward NO. This activated NH_3 then reacts with NO, releasing $\text{V}^{4+}\text{-OH}$, which can then be reoxidized by either NO or O_2 to regenerate $\text{V}^{5+}=\text{O}$. The O_2 speeds up the reaction.

The above observations can be incorporated into a catalytic cycle for the SCR reaction of NO by NH_3 over vanadia-titania catalysts (Scheme 1). According to this scheme, there are essentially two separate catalytic functions on the vanadia-titania catalyst, that is, acid and redox functions. The SCR reaction is initiated by NH_3 adsorption on a $\text{V}^{5+}\text{-OH}$ or Brønsted acid site (step 1 in Scheme 1). The adsorbed NH_3 is then activated by the transfer of a H to the $\text{V}^{5+}=\text{O}$ site, which becomes partly reduced (step 2). Gaseous, or more likely weakly adsorbed, NO subsequently reacts with this activated NH_3 (step 3). In step 4, $\text{V}^{4+}\text{-OH}$ is released together with another intermediate. This intermediate is never seen and therefore probably undergoes rapid decomposition (step 5) to yield the reaction products, N_2 and H_2O , while releasing $\text{V}^{5+}\text{-OH}$ species. In order to complete the catalytic cycle, $\text{V}^{4+}\text{-OH}$ must be oxidized to $\text{V}^{5+}=\text{O}$ (step 6).

Under industrial conditions, one usually has a significant excess of O_2 , and the reoxidation is expected to be fast. Thus, in this case, it may be sufficient to consider mainly steps 1 to 3 in the cycle, which are equivalent to steps I through III in the semiempirical model. Therefore, it also follows that the microkinetic model based on the present steps will have the same form as that discussed in (11)

in the case of excess O_2 and may explain the industrial data satisfactorily.

The fundamental model can account for large changes in the concentrations of the components. This is noteworthy because, in the recent literature, it has been stressed that simplified kinetic treatments and customary approximations have severe limitations when applied to environmental reactions where the removal of polluting compounds to the “ppm” level is required, that is, for ultrapurification or “zero emission” devices (11, 16–18).

The present studies have demonstrated that it is possible to obtain simultaneous in situ information under reaction conditions on the Brønsted and Lewis acid sites, as well as on the vanadia hydroxyl and vanadyl groups. Furthermore, the in situ on-line approach, which is generally applicable for other catalyst systems, allows one to determine the direct relation between the coverages of the adsorbed species and the catalytic rate. This combined information, which has not been available previously, is essential for establishing the detailed mechanism. Such studies also link the fundamental surface chemistry and the industrial reaction rates. An important consequence of the present investigation may be the possibility of bridging science and technology, and of developing new strategies for the “molecular design” of improved catalysts for the removal of NO_x .

REFERENCES AND NOTES

1. M. Takagi, T. Kawai, M. Soma, T. Onishi, K. Tamaru, *J. Catal.* **50**, 441 (1977).
2. M. Inomata, A. Miyamoto, Y. Murakami, *ibid.* **62**, 140 (1980).
3. H. Bosch and F. J. J. G. Janssen, *Catal. Today* **2**, 369 (1988).
4. M. Gasior, J. Haber, T. Machej, T. Czeppe, *J. Mol. Catal.* **43**, 359 (1988).
5. R. A. Rajadhyaksha and H. Knözinger, *Appl. Catal.* **51**, 81 (1989).
6. J. A. Odriozola *et al.*, *J. Catal.* **119**, 71 (1989).
7. G. Ramis, G. Busca, V. Lorenzelli, P. Forzatti, *Appl. Catal.* **64**, 243 (1990).
8. M. Schraml, A. Wokaun, A. Baiker, *J. Catal.* **124**, 86 (1990).
9. N.-Y. Topsøe, *ibid.* **128**, 499 (1991).
10. G. T. Went, L.-J. Leu, R. R. Rosin, A. T. Bell, *ibid.* **134**, 492 (1992).

11. J. A. Dumesic *et al.*, in *New Frontiers in Catalysis, Proceedings of the 10th International Congress on Catalysis, Budapest, Hungary*, L. Guzzi *et al.*, Eds. (Akadémiai Kiadó, Budapest, 1993), p. 1325.
12. See the comments by G. C. Bond and the other discussions following (11).
13. N.-Y. Topsøe and H. Topsøe, *Catal. Today* **9**, 77 (1991).
14. G. Busca, *Langmuir* **2**, 577 (1986).
15. G. T. Went, S. T. Oyama, A. T. Bell, *J. Phys. Chem.* **94**, 4240 (1990).
16. J. R. Rostrup-Nielsen, in *Elementary Reaction Steps in Heterogeneous Catalysis*, R. W. Joyner and R. A. van Santen, Eds. (Kluwer Academic, Dordrecht, Netherlands, 1993), pp. 441–460.
17. M. Boudart, paper presented at the American Chemical Society 1994 spring San Diego meeting, Symposium on Catalytic Reaction Engineering for

- Environmentally Benign Processing.
18. J. A. Dumesic *et al.*, in *The Microkinetics of Heterogeneous Catalysis* (American Chemical Society, Washington, DC, 1993).
 19. I acknowledge helpful discussions with H. Topsøe, J. A. Dumesic, and E. G. Derouane.

23 May 1994; accepted 11 July 1994

The Spatial Structure in Liquid Water

Peter G. Kusalik* and Igor M. Svishchev

Liquid state structure has traditionally been characterized with the radial distribution functions between atoms. Although these functions are routinely available from x-ray diffraction and neutron scattering experiments or from computer simulations, they cannot be interpreted unambiguously to provide the spatial order in a molecular liquid. A direct approach to determining the spatial structure in the liquid state is demonstrated here. Three-dimensional maps representing the local atomic densities are presented for several water models. These spatial maps provide a picture of the short-range order in liquid water which reveals specific details of its local structure that are important in the understanding of its properties.

The unusual physical properties of liquid water, in which its structure plays a key role, have long challenged researchers and have resulted in numerous theoretical and phenomenological models (1–4). The tendency for tetrahedral arrangements in liquid water structure is well established. However, the nature and role of the additional, nontetrahedral coordination that is believed to exist in water have been the subject of extensive debate and speculation (1, 4–6). Although much of the controversy associated with understanding water structure could be resolved if the details of the full three-dimensional (3D) local molecular packing were available, experimental structural studies of water have been restricted to the orientationally averaged (or spatially folded) radial distribution functions (RDFs) between the oxygen (O) and hydrogen (H) atoms, specifically $g_{OO}(r)$, $g_{OH}(r)$, and $g_{HH}(r)$ (7, 8). These functions, which represent the probability of finding a second particle at a separation r from a first, can provide only limited information on the local structure in a molecular system. Unfortunately, computer simulation methods (9, 10) have also relied almost exclusively on RDFs. In a computer simulation study of SPC/E water (11, 12) we overcame the limitations of RDFs by determining the spatial distribution functions (SDFs), $g_{OO}(r, \Omega)$ and $g_{OH}(r, \Omega)$, for oxygen and hydrogen atoms. While still being a contraction of the full two-molecule distribution function, these SDFs span both the radial, r , and

angular, Ω , coordinates of the interatomic separation vector (13) and hence are sufficient to characterize the local 3D packing of molecules. These spatial maps confirm a tetrahedral network pattern of hydrogen (H)-bonded molecules and, for the SPC/E model of liquid water, establish the existence of separate maxima in the local atomic density at “interstitial” (nontetrahedral) positions.

Here we compare the average local structure, as given by the SDF, within several models for liquid water at 25°C and demonstrate that nontetrahedral coordination arises independently of the choice of interaction potential. Hence, we conclude that this structural feature is a general result characteristic of the real system. Along with SPC/E water, the TIP4P potential (14) as well as the recently developed polarizable

point charge (PPC) water model (15) are considered in this computer simulation study; these models and some of their average properties are summarized in Table 1. All three models successfully reproduce some of the bulk properties of liquid water, as can be seen from Table 1, and their RDFs $g_{OO}(r)$, shown in Fig. 1, are all in good agreement with experimental data (7).

The oxygen-oxygen spatial distribution function for the TIP4P and PPC potentials are compared in Fig. 2, where $g_{OO}(r, \Omega)$ have been visualized as 3D oxygen density maps. These SDFs are rich in detail and correctly portray water as a highly structured liquid. We see that the two model liquids share the same principal structural features: the two distinct caps centered directly over the hydrogens of the central molecule due to its two H-bond-accepting neighbors, the single cupped feature below the central molecule due to its two H-bond-donating neighbors, and the two more distant (predominantly blue) features due to additional nontetrahedral coordination. The blue color of this additional coordination emphasizes that these local maxima in oxygen density (which contain roughly one neighbor) occur at separations corresponding to the first minimum in $g_{OO}(r)$ (see Fig. 1). It is these local maxima, which are lost when the angle-averaged RDF is formed, that lead to the elevated pair-density observed around the first minimum in $g_{OO}(r)$. Earlier studies attempting to identify this “interstitial” maximum from the 1D function $g_{OO}(r)$ had led

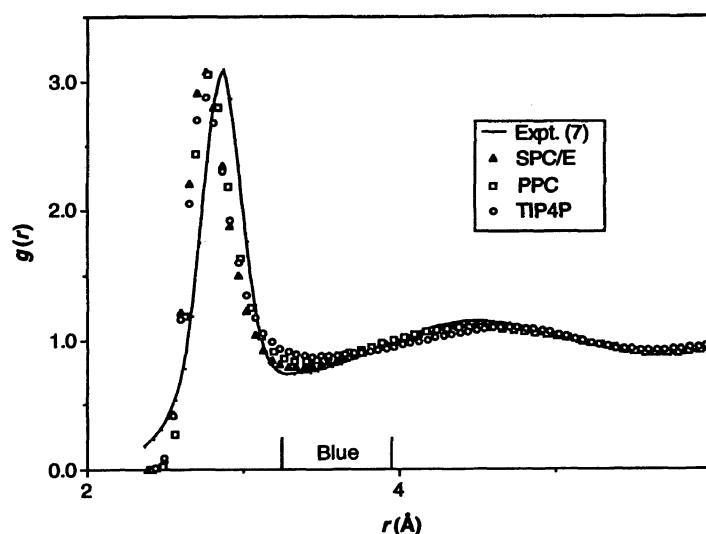


Fig. 1. Comparison of the oxygen-oxygen RDF, $g_{OO}(r)$, for liquid water and the TIP4P, SPC/E, and PPC models for water at 25°C. Also indicated is the range of separations colored blue in Figs. 2 and 4.

Department of Chemistry, Dalhousie University, Halifax, Nova Scotia, B3H 4J3, Canada.

*To whom correspondence should be addressed.